ELSEVIER

Journal of Nuclear Materials 307–311 (2002) 807–810

journal of nuclear materials

www.elsevier.com/locate/jnucmat

Thermal creep of granular breeder materials in fusion blankets

L. Bühler *, J. Reimann

Forschungszentrum Karlsruhe, Associaton FZK-EURATOM, Institut für Kern- und Energietechnik, Postfach 3640, 76021 Karlsruhe, Germany

Abstract

Continuum models for granular materials in fusion blankets are efficient tools for modeling of the nonlinear elastic behavior of pebble beds, granular particle flow caused by shear, volume compaction and hardening. The present paper describes how the material models used in finite element analyses can be extended in order to account additionally for thermally activated creep. The derived material model gives results which are in reasonable accordance with experimental data for pebble beds.

1. Introduction

For a reliable design of fusion blankets with solid breeder and beryllium pebble beds it is important to have validated computational tools for predicting the thermomechanical conditions like stresses, strains or heat transfer [1]. Present solid breeder blankets have in common that the breeder region is split into a number of subregions, alternatingly filled with the breeding ceramic material, e.g. Li_4SiO_4, and the neutron multiplier beryllium, Be. Both materials are used in the form of small pebbles as compact assemblies of granular material. During operation, thermal stresses arise from different thermal expansions and irradiation swelling of the pebble beds and structural materials. Thermal creep of pebble beds is expected to partly release the build-up of stresses and to improve heat transfer due to increased contact areas between the pebbles.

Thermal creep experiments have been performed in an uniaxial compression test facility with pebble beds consisting of FZK-orthosilicate (pebble diameters d between 0.25 and 0.63 mm), and beds consisting of JAERI and CEA-metatitanate pebbles ($d \approx 1$ mm) at temperatures up to 850 °C and maximum uniaxial stresses of 9 MPa [2,3]. For further details about these materials see [4]. A correlation between strain, stress and time has been proposed which we use throughout this paper in the form

$$\dot{\varepsilon}_c = A^*(T)\sigma_{yy}^n t^m, \tag{1}$$

where $\dot{\varepsilon}_c$, σ_{yy} and t are the volumetric creep strain rate, the stress in the y direction, and time, measured in s^{-1}, MPa, and s, respectively. The quantity $A^*(T) = A\exp[-B/T]$ depends on temperature T, measured in K. The coefficients and exponents n and m are shown in Table 1.

In this paper, modelling work is described in order to implement thermal creep in the ABAQUS code used for the description of the thermomechanical behavior of blanket elements. Calculations using the standard routines for thermal creep yield results only for a very short initial period. They fail in predicting the relatively large deformations observed experimentally. For these reasons thermal creep is modelled separately and implemented in a user-defined subroutine. We compare theoretical results with three different types of experiments. One type which is used for calibration is thermal creep during isostatic uniaxial compression. Another type considers the dependence of creep on the temporal load ramps and a third type of experiments considers the stress release due to creep.

* Corresponding author. Tel.: +49-7247 823497; fax: +49-7247 824837.

E-mail address: leo.buehler@iket.fzk.de (L. Bühler).

0022-3115/02/$ - see front matter © 2002 Published by Elsevier Science B.V.
PII: S0022-3115(02)00982-0

Table 1
The creep parameters A, B, n and m for different breeder materials

Material	A	B	n	m
Li_4SiO_4-FZK	2.42	10 220	0.65	−0.8
Li_2TiO_3-CEA	0.12	7576	0.65	−0.82
Li_2TiO_3-JAERI	0.07	6947	0.65	−0.81

2. Creep in solid and granular materials

Thermal creep of solid ceramic materials under compression exhibits a primary and a secondary creep phase [5]. The secondary creep phase with constant strain rate

$$\dot{\varepsilon} \sim \sigma^{\alpha} \tag{2}$$

is active over most of the time during experiments. Moreover, many materials do not exhibit a primary phase. Therefore we do not distinguish in the following between primary and secondary creep.

In a granular bed, creep will not occur with the same magnitude in the whole material. Especially in the vicinity of surfaces where granular particles are in contact with each other we have the highest stresses so that the magnitude of the creep strain rate $\dot{\varepsilon}$ is largest there. During creep the contact areas increase. This reduces the local stresses for the same externally applied load so that $\dot{\varepsilon}$ is decreased. In addition, initial gaps may close during creep compaction. This fact creates new contacts which transmit a fraction of the load and decreases the average stress per contact surface, resulting in lower creep strain rate $\dot{\varepsilon}$ with progressing time.

Motivated by the experimental observations summarized in Eq. (1) we therefore use the more general law for volumetric creep strain

$$\dot{\varepsilon}_{\mathrm{c}} = A^{*}(T) p^{n} t^{m}, \tag{3}$$

with a magnitude A depending on temperature T. Here, the scalar $p = -\mathrm{trace}(\boldsymbol{\sigma})$ stands for the pressure stress measured in MPa.

Let us support this creep law with some heuristic arguments. Suppose a granular particle is in contact with its neighboring particles at the contact areas at which the force $\mathbf{F}$ is transmitted. The situation is depicted in Fig. 1. In the following we denote the average compressive stress as $p \sim F/d^2$. During creep the radius of the contact area and the contact surface increase as $\varepsilon^{1/2} d$ and εd^2, respectively, where ε is proportional to the volumetric strain of the granular bed. In the contact region the stress is related to the compressive granular load as $\sigma \sim F/\varepsilon d^2 \sim (1/\varepsilon)p$. This yields with Eq. (2), $\dot{\varepsilon} \sim ((1/\varepsilon)p)^{\alpha}$ and after integration

$$\varepsilon \sim p^{\alpha/(\alpha+1)} t^{1/(\alpha+1)} \quad \text{or} \quad \dot{\varepsilon} \sim p^{\alpha/(\alpha+1)} t^{-\alpha/(\alpha+1)}. \tag{4}$$

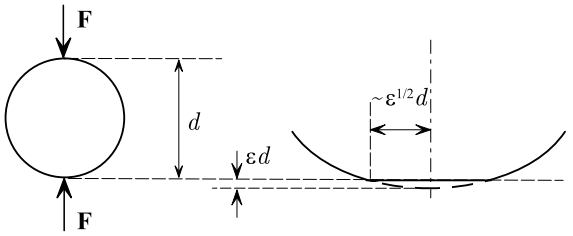

Fig. 1. Sketch of a particle in creeping contact.

This equation shows that even if a solid material has a constant creep velocity, a granular body with particles of the same material will have a different behavior. The exponent m may be extracted from granular experiments to be close to $m_{\mathrm{exp}} = -0.82$. This means that the exponent α would have values about $\alpha \approx 4$, which is in the range of ceramic materials under compression where e.g. $\alpha = 3.65$ for silicon carbide [5]. The assumptions introduced so far oversimplify the real situation. This is manifested by an inaccurate prediction of the pressure dependence in Eq. (4) where the model would predict $n = -m$ which overestimates the stress exponent $n = 0.65$ observed in the experiment. The best agreement between numerical calculations and experiments was obtained by using an exponent for pressure as $n = 0.71$. The deficiency of the model may be caused by the fact that the stress at the contact surface is not uniform and because the contact areas are estimated from simple geometric considerations without reference to precise deformations. We therefore do not use Eq. (4) but chose the more general creep law, Eq. (3). We show that the degrees of freedom are sufficient to reproduce well the data obtained in creep experiments.

3. Analysis and experiments

Plastic creep flow is determined by the strain rate tensor

$$\dot{\mathbf{e}} \sim \frac{\partial G_{\mathrm{c}}}{\partial \boldsymbol{\sigma}}, \quad \text{where } G_{\mathrm{c}} = \sqrt{p^2 + (rq)^2} \tag{5}$$

is the consolidation creep potential determined by the pressure stress p and the Mises equivalent stress q. For a lack of knowledge we chose $r = 1$ and assume orthotropic creep deformations. Normalization such that $\dot{e}_{xx} + \dot{e}_{yy} + \dot{e}_{zz} = \dot{\varepsilon}_{\mathrm{c}}$ finally yields

$$\dot{e}_{xx} = \frac{\dot{\varepsilon}_{\mathrm{c}}}{6}\left(9\frac{\sigma_{xx}}{p} + 7\right), \tag{6}$$

and equivalent expressions for the components $\dot{e}_{yy}$ and $\dot{e}_{zz}$. These strain rates cannot be used directly for a code input in the ABAQUS creep laws. However, the user subroutine UEXPAN foreseen for modelling of user-

defined incremental strain allows us to define Δe_{xx}, Δe_{yy}, and Δe_{zz}. This is done by integration of Eq. (6) over the time increment Δt [6]. The latter reference shows in addition how creep contributes to hardening, an effect that is important for successive increase of the load. Figs. 2 and 3 show calculations of thermal creep during uniaxial compression tests in comparison with a typical experiment at 800 °C. For $t < t_0 = 5$ min the load is increased gradually and kept constant at $\bar{\sigma}_{yy} = 4.3$ MPa for $t_0 < t < 5600$ min. Then, the load is increased in a second step to $\bar{\sigma}_{yy} = 8.58$ MPa and kept constant for $5605 < t < 12850$ min. A comparison with the experimental data at 800 °C shows here a perfect agreement also for the second step after the external load is raised. Thermal creep is practically unimportant for temperature near 400 °C or lower.

We have seen already from Fig. 2 that for high temperatures creep gives an essential contribution to the strain magnitude already during the initial period when the load is applied. This fact is investigated experimentally and compared with theoretical predictions. In the following we use for the stress increase different load ramps between 0.15 and 4.7 MPa/min and show the results in Fig. 4. We observe large creep strain during the loading period if the load ramp is very slow, i.e. when the material finds enough time to deform. For fast ramps (shorter time) the deformation due to creep is smaller. Fig. 4 shows a reasonable agreement between experiments (lines) and calculations (symbols). For a comparison a loading cycle at ambient temperature has been added to the diagram. For low temperature, creep during the loading period is negligible and results become therefore independent of the load ramps. Note, during experiments one observes typically a very small (negligible) stress increase with initial volumetric strain ε_0. The values of ε_0 depend rather on the initial conditions than on the applied load. This behavior may be explained by a rearrangement of particles near the walls or in the bed. The experimental results plotted in Fig. 4 show the axial load $\bar{\sigma}_{yy}(\varepsilon_{\mathrm{vol}} - \varepsilon_0)$ where we used $\varepsilon_0 = 0.003$, 0.0002 and 0.001, for the cases with 0.15, 2.8, 4.7 MPa/min, and for no-creep, respectively.

The creep behavior as a function of time is shown in Fig. 5 for the two load ramps of 0.17 and 2.8 MPa/min. After the axial stress reaches a level of 6.5 MPa this magnitude is held constant for the rest of the creep experiment. It can be seen from the figure that the creep strain rates differ during the loading period and even some time later. However, on a longer time scale the remaining difference becomes insignificant.

In applications for fusion blankets the load is established by differences in thermal expansion coefficients between the granular material and the confining walls. Under such constraints thermal creep will relax stresses

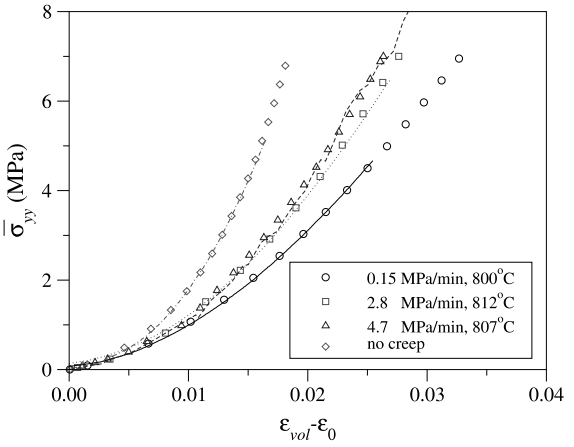

Fig. 4. Vertical component of stress versus reduced strain $\varepsilon_{\mathrm{vol}} - \varepsilon_0$ at various stress ramps.

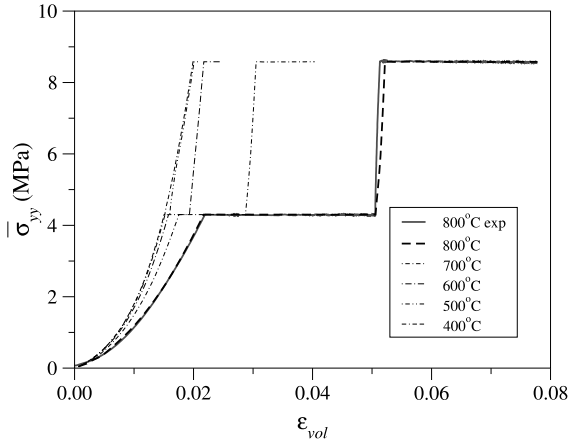

Fig. 2. Vertical component of stress versus volumetric strain at various temperatures.

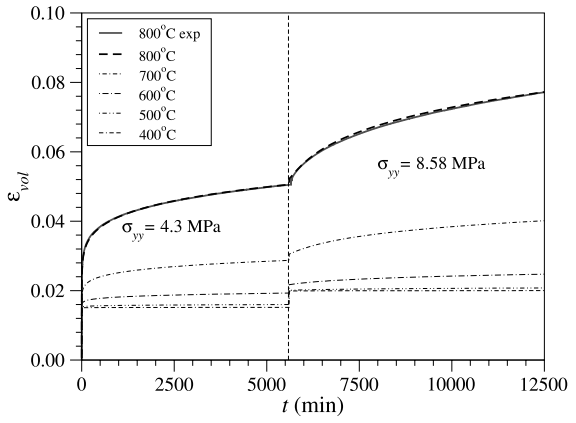

Fig. 3. Volumetric strain versus time at various temperatures.

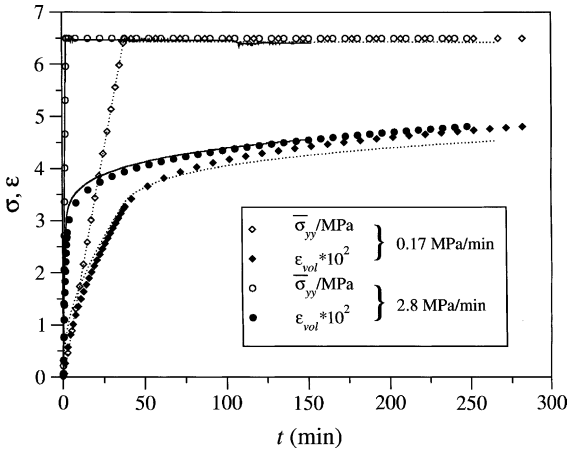

Fig. 5. Influence of different load ramps on long-term thermally activated creep.

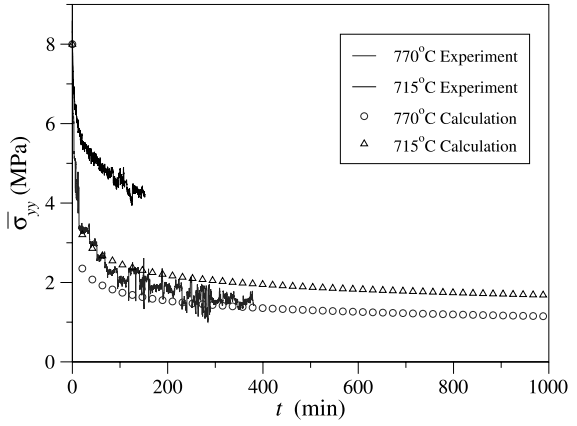

Fig. 6. Stress release by thermal creep. Vertical component of stress as a function of time.

during the operation of the blanket. In order to investigate such effects the third type of experiments has been performed in which the granular bed has been compressed up to $\sigma_{yy} = 8$ MPa to simulate the thermally induced loads. Then the axial stress has been manually controlled in order to keep the piston in a constant position while the vertical force (vertical stress) is recorded (see Fig. 6). This manual control was crucial in a sense that vertical stress amplitudes up to 1 MPa were required in order to reestablish the initial position of the plate. The agreement between theory and experiment in the initial stage is not satisfactory. However, for 770 °C the experimental data approach the theoretical one for the long-term behavior. Typically creep refers to much longer duration (months, years). From the experiment mentioned above it can be seen that after a time less than one hour the stress is released to a fraction of the initial value. This means that at higher temperatures thermal stresses do not cause severe problems if the thermal ramps are slow enough that stresses can be released by thermal creep. This effect was demonstrated already after 400 min and the experiment was terminated. For high temperatures a decrease of stress according to a power law $\sigma_{yy} \sim t^{-0.2}$ is observed.

4. Conclusions

Thermal creep of granular breeder materials has been investigated. Experiments performed at elevated temperatures close to the operating temperatures in fusion blankets show that the creep strain reaches values as large as the elastic and plastic granular deformations. The time after which these large creep deformations occur is relatively small (some hours). This has the consequence that thermally induced loads in the pebble beds or loads due to irradiation swelling are continuously released by creep of the breeder material and should not cause severe problems at high temperatures. Continuum models are efficient means for the determination of the mechanical behavior of granular breeder materials in fusion blankets. Such models account for various effects such as nonlinear elasticity, granular flow of particles due to shear or consolidation, and thermally activated creep. The modelling of thermally activated creep is possible by using a modified cap-creep potential. The new creep potential has been implemented in a user-defined subroutine and yields results which agree well with experimental data for pebble beds.

References

[1] L. Boccaccini, Forschungszentrum Karlsruhe, Report FZKA 6402, 2000.
[2] J. Reimann, G. Wörner, Fus. Eng. Des. 58&59 (2001) 647.
[3] J. Reimann, G. Wörner, Thermal creep of ceramic breeder pebble beds, in: 9th International Workshop on Ceramic Breeder Blanket Interactions, University of Tokyo, 2000, p. 95.
[4] J. Reimann, L. Boccaccini, M. Enoeda, A.Y. Ying, Fus. Eng. Des. 61–62 (2002), to appear in Proceedings of ISFNT-6, San Diego, USA, 7–12 April 2002.
[5] D. Munz, T. Fett, Ceramics: Mechanical Properties, Failure Behaviour, Materials Selection, Springer-Verlag, Berlin/Heidelberg, 1999.
[6] L. Bühler, Forschungszentrum Karlsruhe, Report FZKA 6561, 2001.